Supplementary Information: The aerosol pathway is crucial for observationally constrained climate sensitivity and anthropogenic forcing

Ragnhild Bieltvedt Skeie[1], Magne Aldrin[2], Terje K. Berntsen[3], Marit Holden[2], Ragnar Bang Huseby[2], Gunnar Myhre[1], Trude Storelvmo[3]

[1]CICERO Center for International Climate Research, P.O. Box 1129 Blindern, 0318 Oslo, Norway

[2]Norwegian Computing Center, P.O. Box 114 Blindern, 0314 Oslo, Norway

[3]Department of Geosciences, University of Oslo, P.O. Box 1047 Blindern, 0316 Oslo, Norway

Supplementary Tables

Table S1: ECS_{inf} posteriori mean, median, 5 and 95 percentiles for the different analysis and sensitivity tests. These numbers correspond to the values in Fig. 1.

	Mean	Median	5perc	95perc
Skeie18, AR5 prior	1.95	1.85	1.17	3.07
Update obs. end year 2014	1.99	1.92	1.31	2.92
Replace AR5 prior with AR6	1.99	1.94	1.38	2.79
End year 2019	2.02	1.98	1.43	2.76
Base	2.12	2.09	1.50	2.87
Replace AR6 prior with AR6 extended	2.19	2.15	1.52	2.98
Update obs. end year 2019	2.19	2.16	1.53	2.94
Base extended (end year 2022)	2.22	2.20	1.55	3.00
Smooth	2.16	2.12	1.53	2.90
Linear1750to1900	2.10	2.06	1.48	2.83
Weaker1900to1950	2.12	2.09	1.50	2.87
Stronger1900to1950	2.07	2.04	1.47	2.77
Weaker1950to1980	2.22	2.17	1.52	3.09
Stronger1950to1980	1.97	1.94	1.41	2.60
StrongerWeaker1980to2019	1.95	1.93	1.44	2.55
Stronger1980to2019	2.18	2.14	1.50	3.00
LinWeaker2014to2019	2.06	2.03	1.49	2.73
Linear1950to1990	2.25	2.21	1.56	3.09
Linear1950to2000	2.34	2.28	1.57	3.33
Linear1950to2010	2.33	2.27	1.54	3.36
Linear1950to2019	2.11	2.07	1.44	2.91
Linear1950to1980 then flat	2.35	2.29	1.58	3.29
Linear1950to1990 then flat	2.41	2.34	1.55	3.50
Linear1950to2000 then flat	2.46	2.36	1.54	3.65
Unc. in 1950 and 2014 independent	2.25	2.17	1.44	3.32

Table S2: Transient Climate Response (TCR) posteriori mean, median, 5 and 95 percentiles for the different analysis and sensitivity tests. These numbers correspond to the values in Fig. S9.

	Mean	Median	5perc	95perc
Skeie18, AR5 prior	1.43	1.38	0.94	2.06
Update obs. end year 2014	1.45	1.41	1.02	1.99
Replace AR5 prior with AR6	1.51	1.48	1.10	2.02
End year 2019	1.54	1.52	1.14	2.02
Base	1.54	1.52	1.12	2.00
Replace AR6 prior with AR6 extended	1.57	1.56	1.14	2.06
Update obs. end year 2019	1.57	1.56	1.14	2.04
Base extended (end year 2022)	1.59	1.57	1.14	2.07
Smooth	1.56	1.54	1.15	2.02
Linear1750to1900	1.51	1.50	1.11	1.96
Weaker1900to1950	1.53	1.52	1.12	1.99
Stronger1900to1950	1.51	1.50	1.11	1.94
Weaker1950to1980	1.58	1.56	1.14	2.09
Stronger1950to1980	1.45	1.44	1.07	1.87
StrongerWeaker1980to2019	1.45	1.44	1.09	1.85
Stronger1980to2019	1.56	1.54	1.13	2.05
LinWeaker2014to2019	1.51	1.49	1.12	1.93
Linear1950to1990	1.60	1.59	1.17	2.09
Linear1950to2000	1.64	1.62	1.16	2.19
Linear1950to2010	1.63	1.61	1.14	2.19
Linear1950to2019	1.53	1.51	1.09	2.02
Linear1950to1980 then flat	1.65	1.64	1.17	2.19
Linear1950to1990 then flat	1.67	1.65	1.15	2.26
Linear1950to2000 then flat	1.69	1.66	1.15	2.33
Unc. in 1950 and 2014 independent	1.58	1.55	1.09	2.18

Table S3:Total anthropogenic ERF prior and posteriori mean, median, 5 and 95 percentiles for the different analysis and sensitivity tests for the end year. These numbers correspond to the values in Fig. 2b.

	mean	median	5perc	95perc
Prior:				
AR5 prior 2014	2.38	2.4	1.23	3.45
AR6 prior 2014	2.36	2.36	1.55	3.17
AR6 prior 2019	2.72	2.72	1.96	3.48
AR6 extended prior 2019	2.63	2.64	1.8	3.44
AR6 extended prior 2022	2.91	2.91	2.19	3.63
Posterior:				
Skeie18, AR5 prior	2.46	2.44	1.44	3.54
Update obs. end year 2014	2.59	2.56	1.72	3.53
Replace AR5 prior with AR6	2.94	2.93	2.40	3.51
End year 2019	3.22	3.21	2.69	3.77
Base	3.15	3.14	2.64	3.68
Replace AR6 prior with AR6 extended	3.00	2.99	2.48	3.55
Update obs. end year 2019	2.97	2.96	2.48	3.50
Base extended (end year 2022)	3.17	3.16	2.69	3.67
Smooth	3.12	3.11	2.62	3.65
Linear1750to1900	3.11	3.10	2.60	3.66
Weaker1900to1950	3.16	3.16	2.67	3.69
Stronger1900to1950	3.16	3.15	2.65	3.69
Weaker1950to1980	3.06	3.05	2.52	3.64
Stronger1950to1980	3.28	3.27	2.78	3.78
StrongerWeaker1980to2019	3.29	3.29	2.81	3.79
Stronger1980to2019	3.19	3.18	2.69	3.71
LinWeaker2014to2019	3.37	3.36	2.91	3.83
Linear1950to1990	3.02	3.01	2.50	3.58
Linear1950to2000	2.92	2.90	2.35	3.53
Linear1950to2010	2.81	2.80	2.19	3.49
Linear1950to2019	2.82	2.81	2.15	3.54
Linear1950to1980 then flat	2.79	2.77	2.23	3.41
Linear1950to1990 then flat	2.71	2.69	2.10	3.39
Linear1950to2000 then flat	2.64	2.62	1.98	3.36
Unc. in 1950 and 2014 independent	3.14	3.13	2.57	3.74

Table S4: Total aerosol ERF prior and posteriori mean, median, 5 and 95 percentiles for the different analysis and sensitivity tests for the end year. These numbers correspond to the values in Fig 3b.

	mean	median	5perc	95perc
Prior:				
AR5 prior 2014	-0.94	-0.90	-1.92	-0.08
AR6 prior 2014	-1.20	-1.19	-1.91	-0.49
AR6 prior 2019	-1.06	-1.06	-1.71	-0.42
AR6 extended prior 2019	-1.17	-1.16	-1.89	-0.48
AR6 extended prior 2022	-0.98	-0.98	-1.58	-0.41
Posterior:				
Skeie18, AR5 prior	-0.89	-0.87	-1.82	-0.01
Update obs. end year 2014	-0.80	-0.78	-1.64	0.00
Replace AR5 prior with AR6	-0.67	-0.67	-1.13	-0.19
End year 2019	-0.62	-0.62	-1.03	-0.20
Base	-0.68	-0.68	-1.07	-0.28
Replace AR6 prior with AR6 extended	-0.85	-0.85	-1.26	-0.41
Update obs. end year 2019	-0.87	-0.87	-1.26	-0.46
Base extended (end year 2022)	-0.76	-0.77	-1.10	-0.41
Smooth	-0.71	-0.71	-1.10	-0.31
Linear1750to1900	-0.71	-0.71	-1.12	-0.29
Weaker1900to1950	-0.66	-0.66	-1.04	-0.27
Stronger1900to1950	-0.66	-0.67	-1.05	-0.26
Weaker1950to1980	-0.74	-0.75	-1.17	-0.29
Stronger1950to1980	-0.56	-0.56	-0.92	-0.20
StrongerWeaker1980to2019	-0.54	-0.54	-0.88	-0.20
Stronger1980to2019	-0.63	-0.64	-1.01	-0.24
LinWeaker2014to2019	-0.46	-0.46	-0.72	-0.19
Linear1950to1990	-0.79	-0.80	-1.22	-0.35
Linear1950to2000	-0.88	-0.88	-1.35	-0.38
Linear1950to2010	-0.96	-0.97	-1.48	-0.40
Linear1950to2019	-0.94	-0.94	-1.51	-0.35
Linear1950to1980 then flat	-1.00	-1.01	-1.47	-0.51
Linear1950to1990 then flat	-1.06	-1.07	-1.58	-0.51
Linear1950to2000 then flat	-1.11	-1.12	-1.66	-0.52
Unc. in 1950 and 2014 independent	-0.80	-0.81	-1.21	-0.36

Supplementary Figures

Supplementary Figures Methods

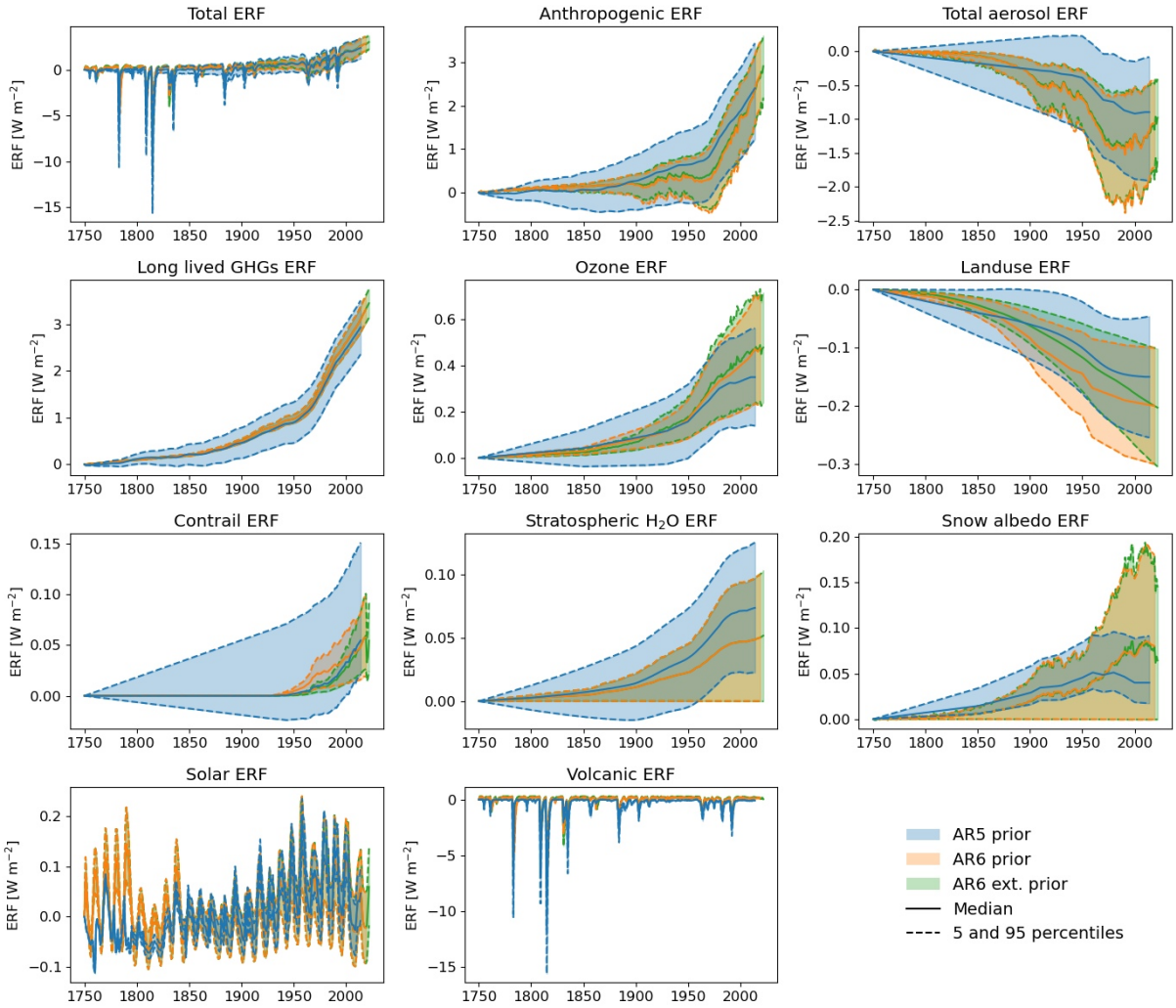

Figure S1: Prior ERF timeseries for the different forcing components. The shading and the dashed lines indicate the 90 % uncertainty ranges, and the solid line is the median ERF time series. Values from IPCC AR5 (Myhre et al., 2013) with historical uncertainty as implemented in Skeie et al. (2018) are shown in blue, from IPCC AR6 (Forster et al., 2021) in orange and IPCC AR6 extended to 2022 (Forster et al., 2023) in green. The components plotted here are the components included in IPCC AR5. For AR6 and AR6 extended the ERF for CO_2, CH_4, N_2O and other well mixed greenhouse gases are used separately and the sum of these are shown here as Long lived GHGs. In AR6 and AR6 extended the total aerosol ERF are split between ERFari and ERFaci but the sum is shown here for comparison with AR5. Note that the scale on y-axis differ and that uncertainties in contrail forcing was incorrectly implemented in Skeie et al. (2018) as ERF should have been zero before 1930.

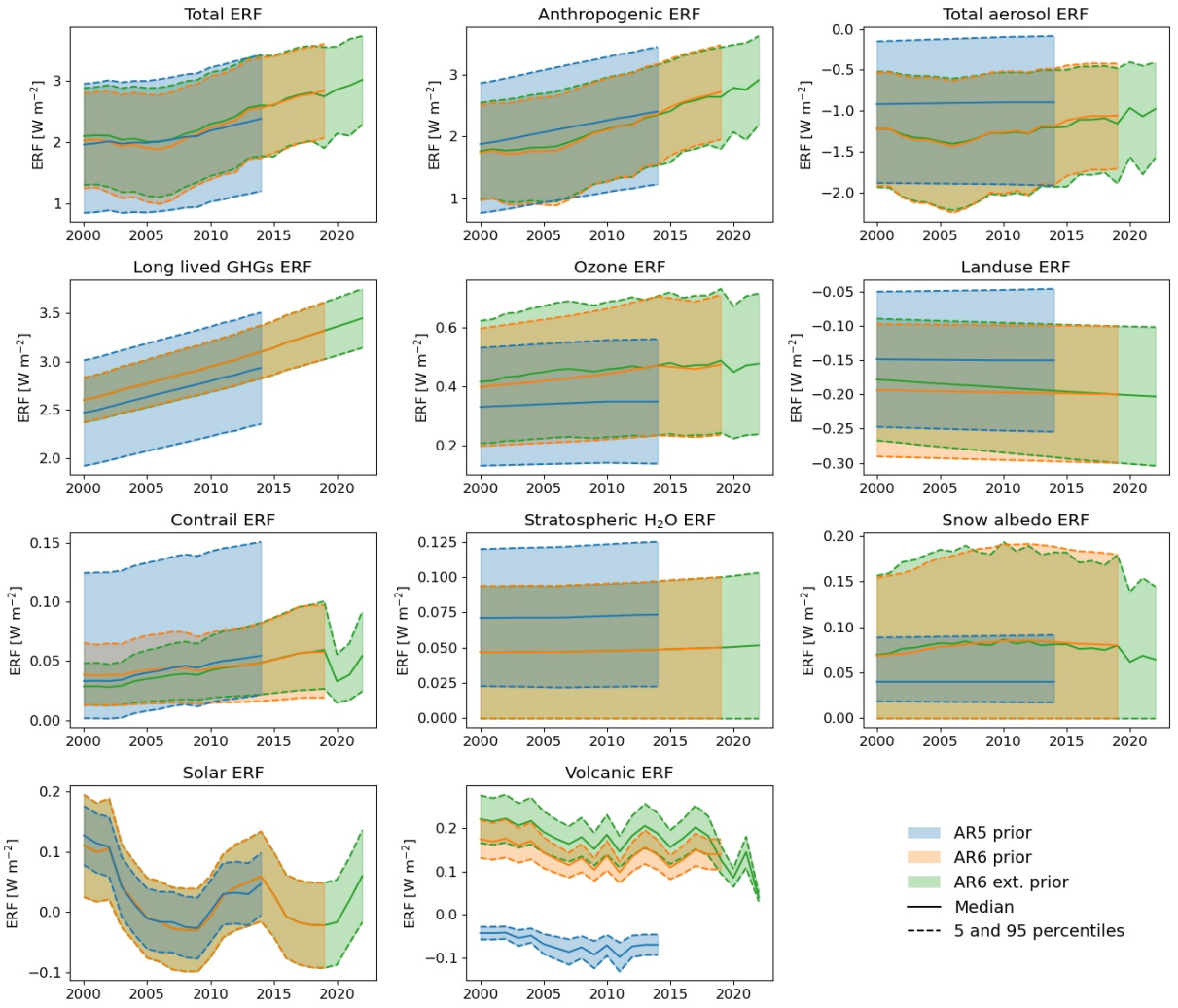

Figure S2: Same as Fig. S1, but ERF priors for a shorter period is shown.

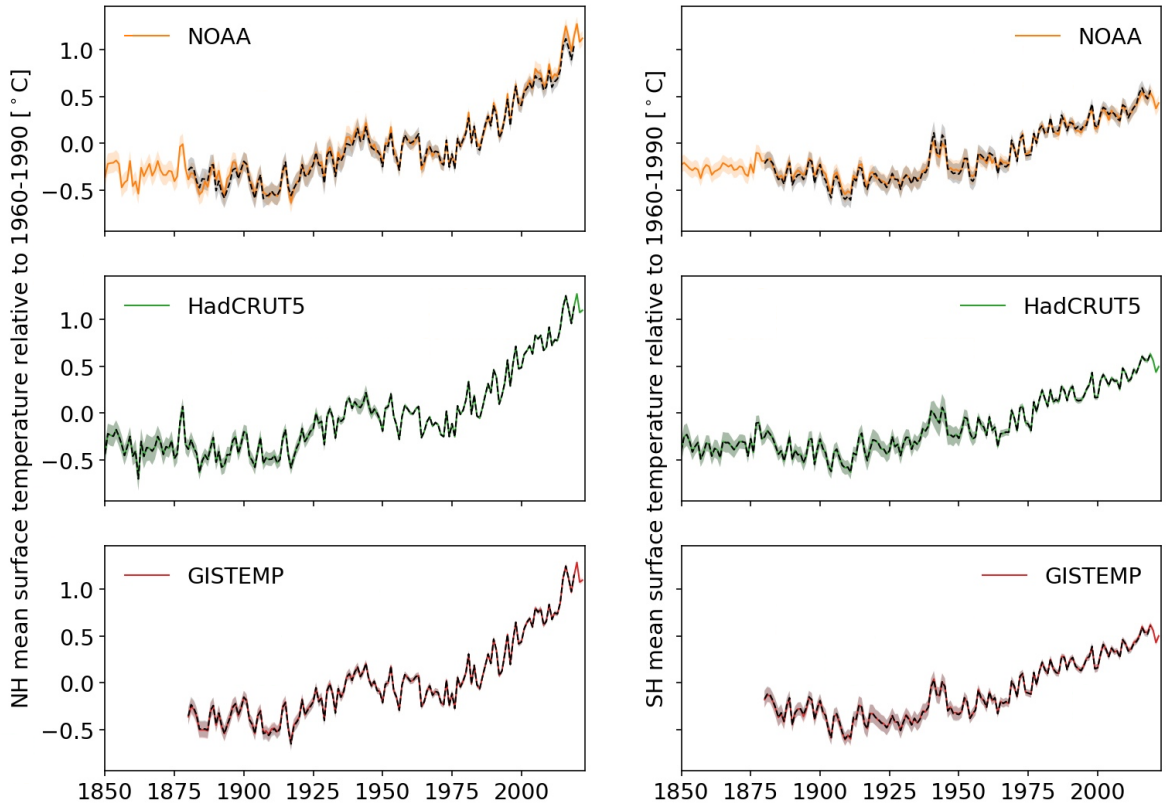

Figure S3. Hemispheric annual mean surface temperature for the three different observational based series (Table A2) used in the estimation. Temperatures are plotted relative to a 1960-1990 baseline and the shading indicates uncertainty of one standard deviation. The colored lines are the updated values to 2022 used in "Base extended", while the black dashed lines are the values up to 2019 used in "Base".

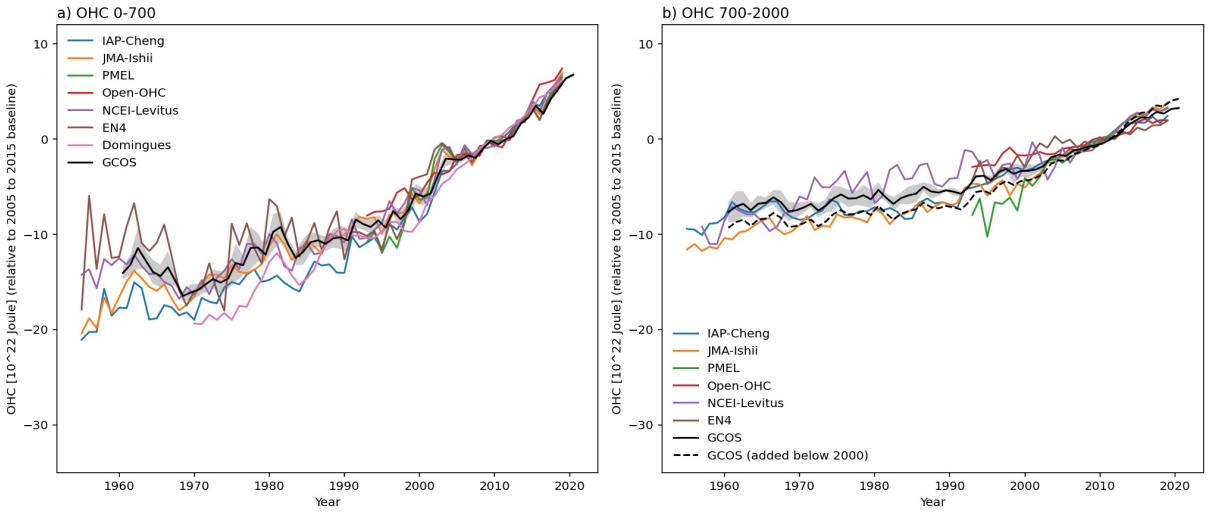

Figure S4: The observational based series for OHC used in "Base" as listed in Table A2. OHC anomalies (relative to reference period 2005 to 2015) for upper 700 meter in a) and 700 meters to 2000 meters in b). GCOS data from von Schuckmann et al. (2023) is added to the figure. The dashed black line in b) is GCOS data below 700 meters that includes OHC below 2000 meters.

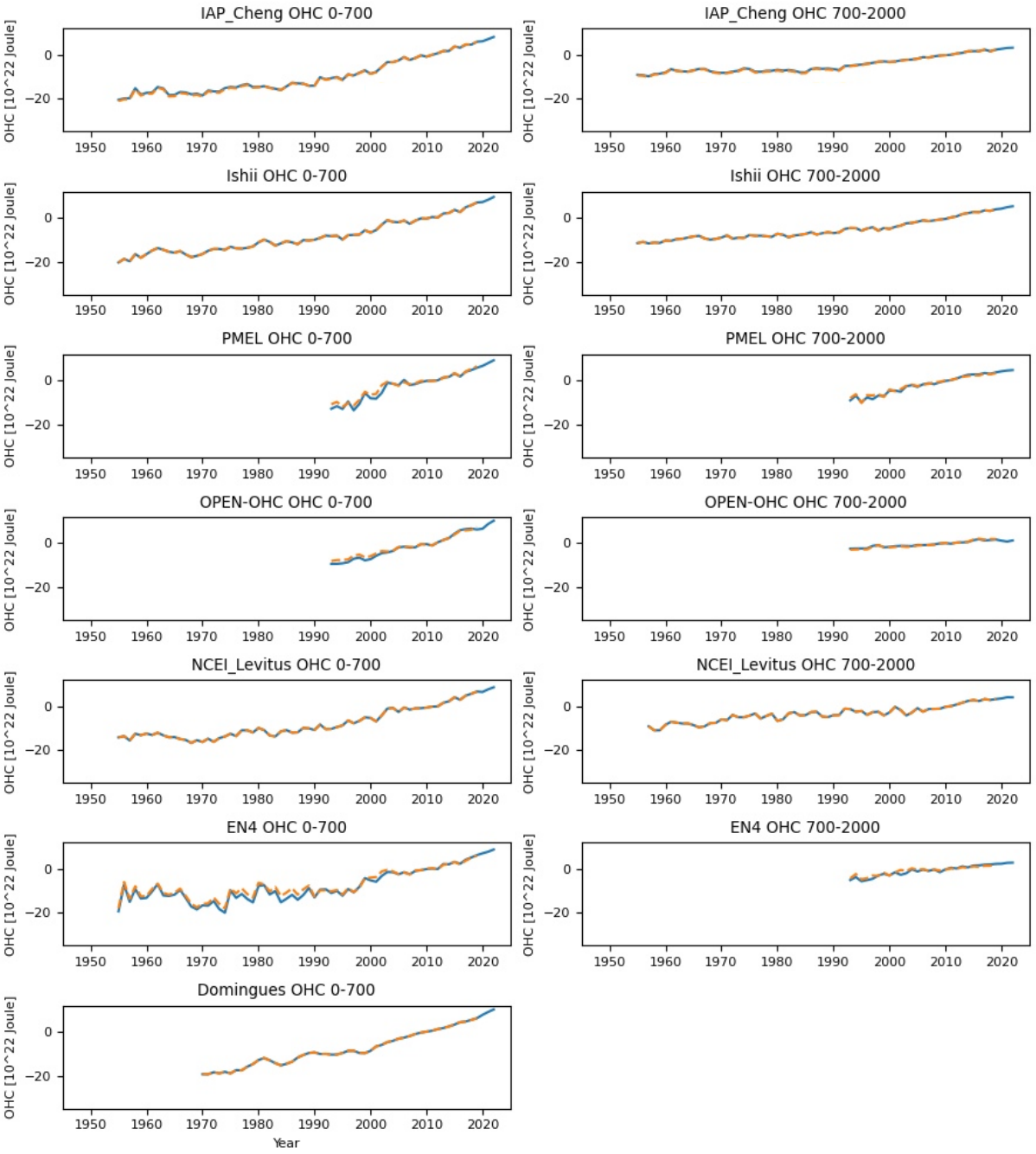

Figure S5: Anomalies for observed ocean heat content. OHC 0-700 meters (left) and OHC 700-2000 meters (right) for the different time series (Table A2). The blue lines are the updated data up to 2022 used in "Base extended" while the dashed orange lines are the data up to 2019 used in "Base". The OHC data are plotted relative to a 2005 to 2015 baseline.

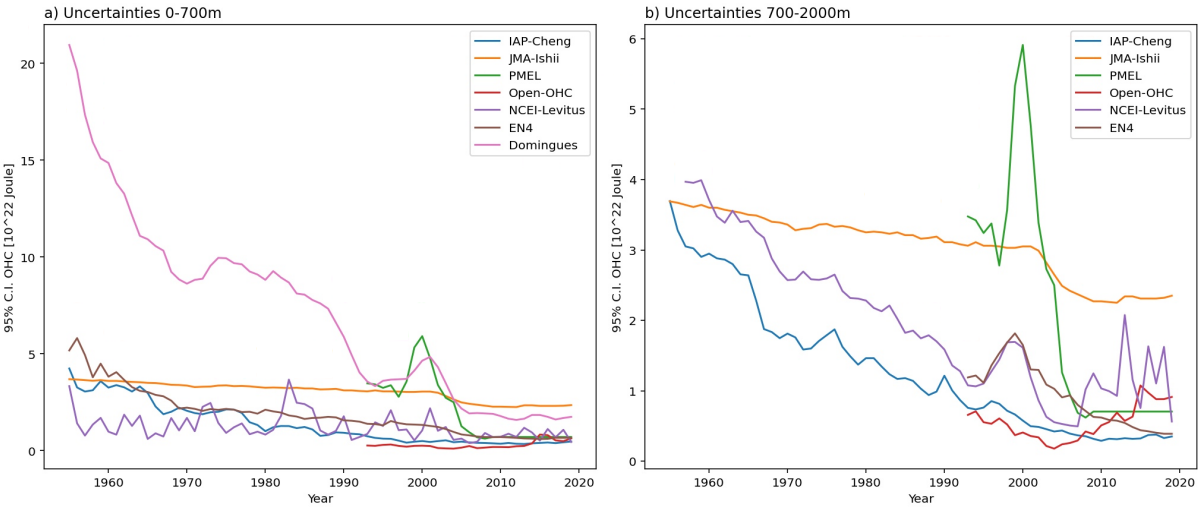

Figure S6: The uncertainties in the observational based series for OHC (Table A2). In a) for the upper 700 meters and in b) for 700 to 2000 meters.

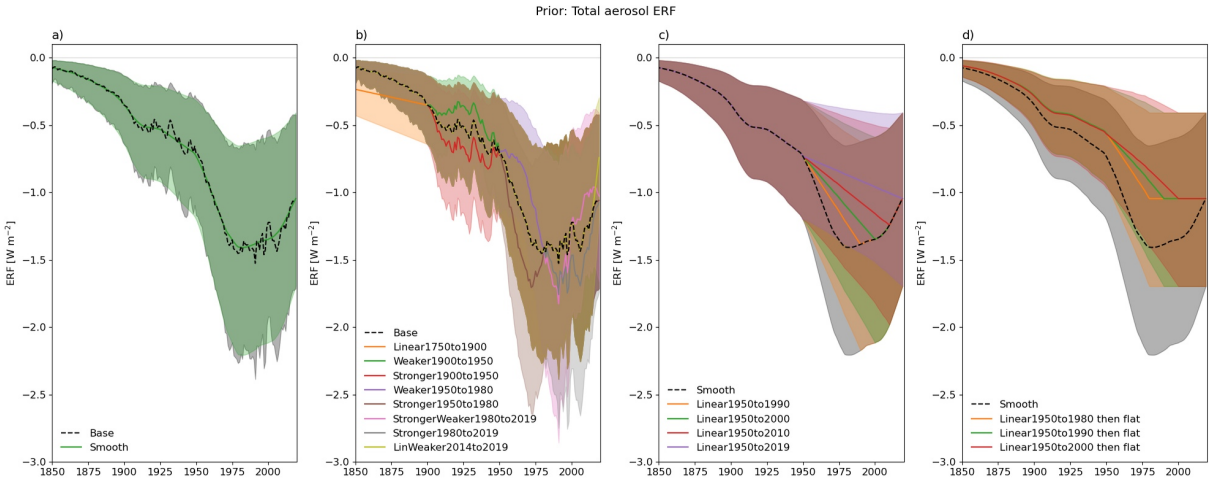

Figure S7: Prior total aerosol ERF time series for "Base" and for the aerosol ERF sensitivity tests. The mean value is indicated by a line and 90% uncertainty range by the shading. Both the ERFari and ERFaci are adjusted in the sensitivity tests, and the sensitivity test are described in Table A3.

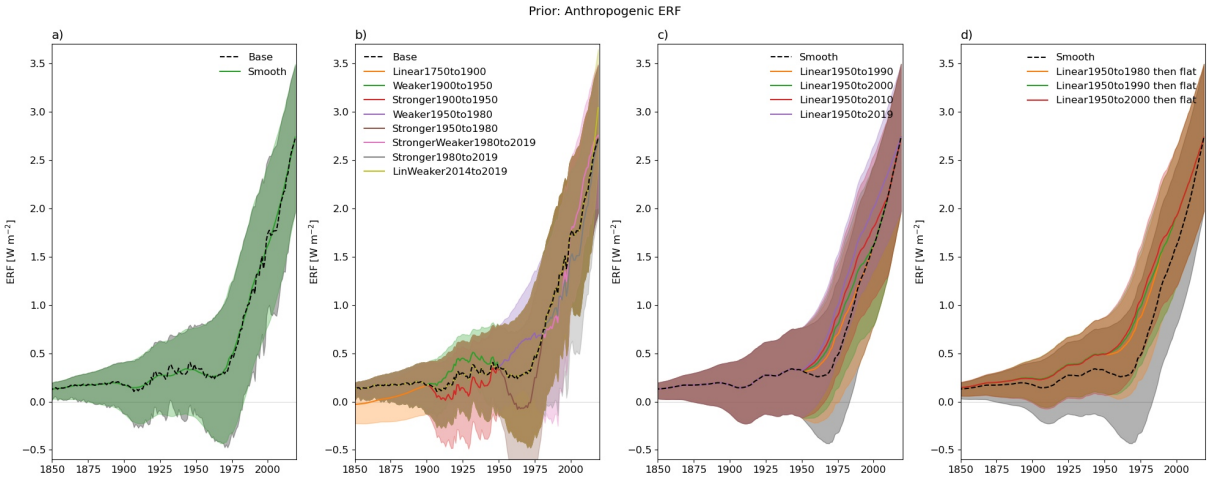

Figure S8: Same as Fig. S7 but for total anthropogenic ERF.

Supplementary Figures Results

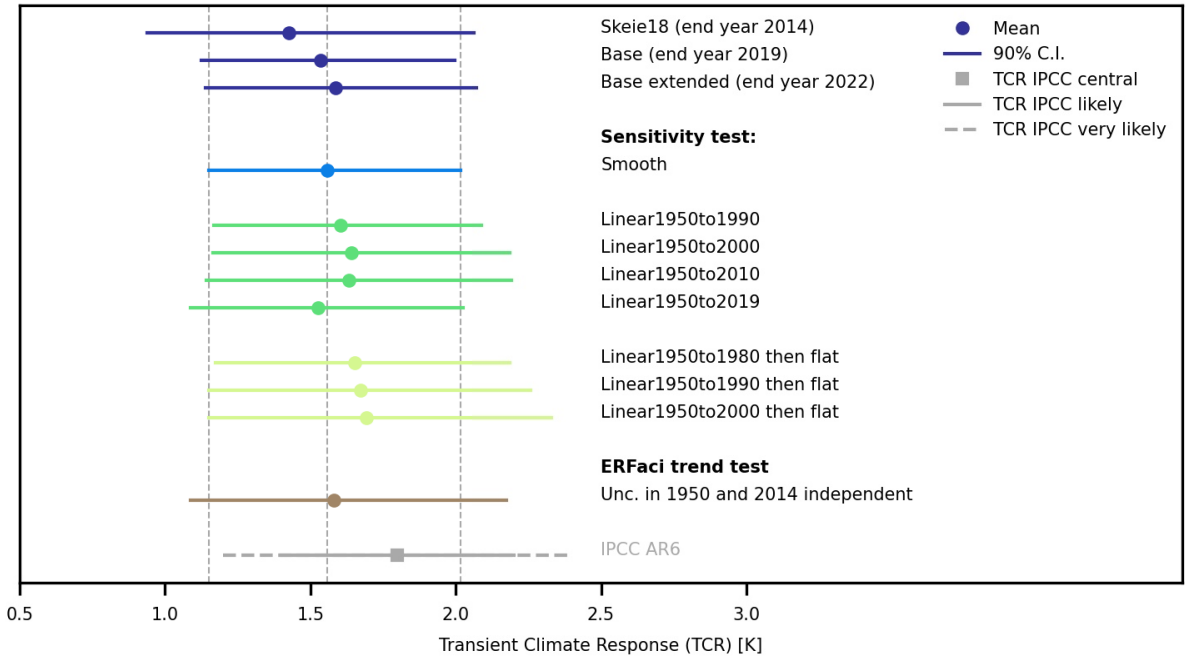

Figure S9: Posterior Transient Climate Response (TCR) for the different analyses and sensitivity tests. The 90% C.I. is indicated by a solid line and the mean values as a dot. The vertical lines indicate the posterior mean value and 90% C.I. for "Smooth", as it is used as a starting point for the "Linear" sensitivity tests shown. The TCR central estimate, and likely (66% probability) and very likely (90% probability) ranges from IPCC AR6 (Forster et al., 2021) are shown in grey colours at the bottom. The posterior mean, median and 5 and 95 percentiles are presented in Table S2.

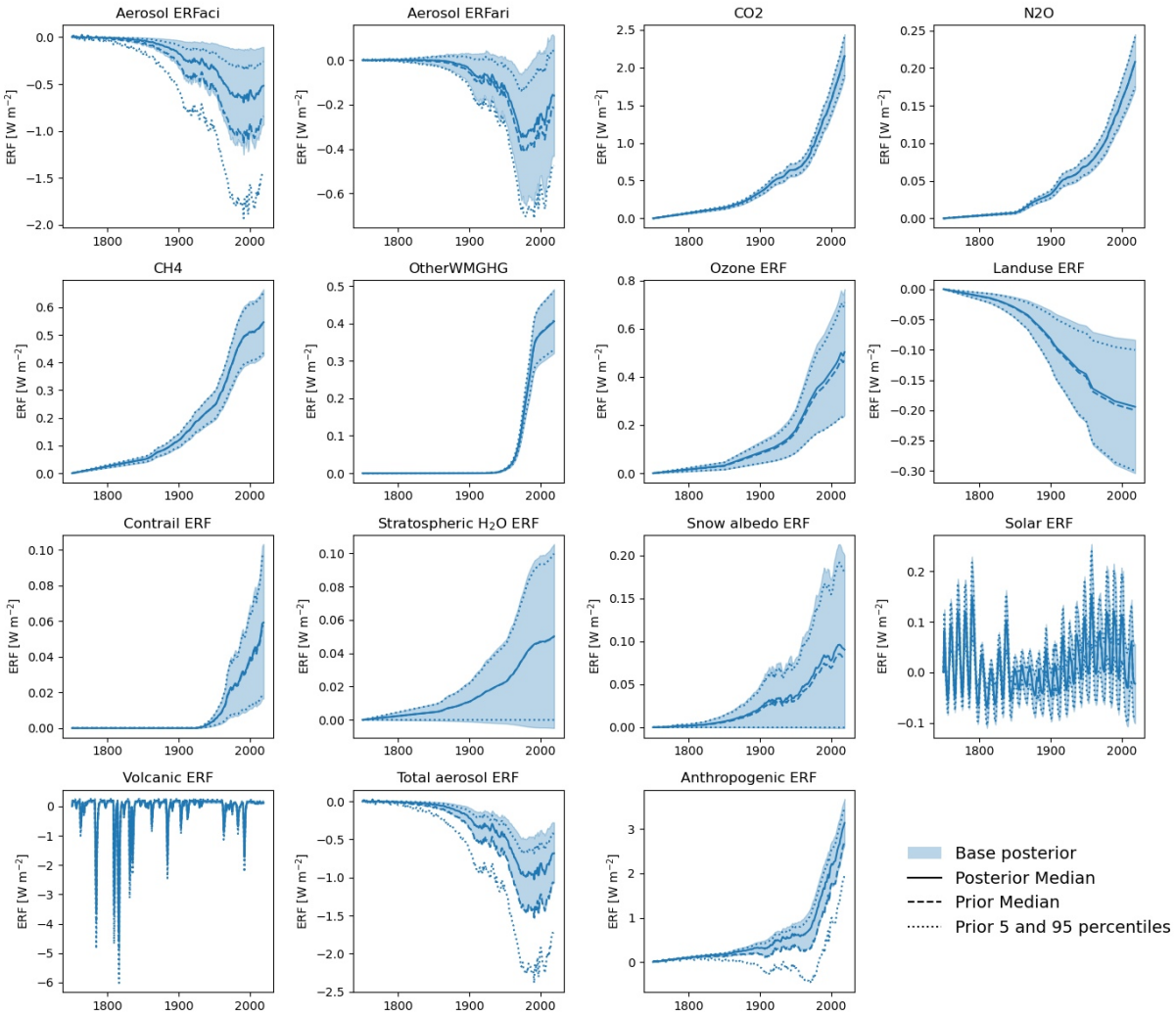

Figure S10: Prior and posteriori distribution for the historical ERFs for all forcing components included in "Base". The prior median is shown as dashed line and the 5th and 95th percentile as dotted lines. The posterior median is shown as solid line and the 5th to 95th range as shading. In addition, the total aerosol ERF which is the sum of Aerosol ERFaci and Aerosol ERFari as well as the Anthropogenic ERF is shown.

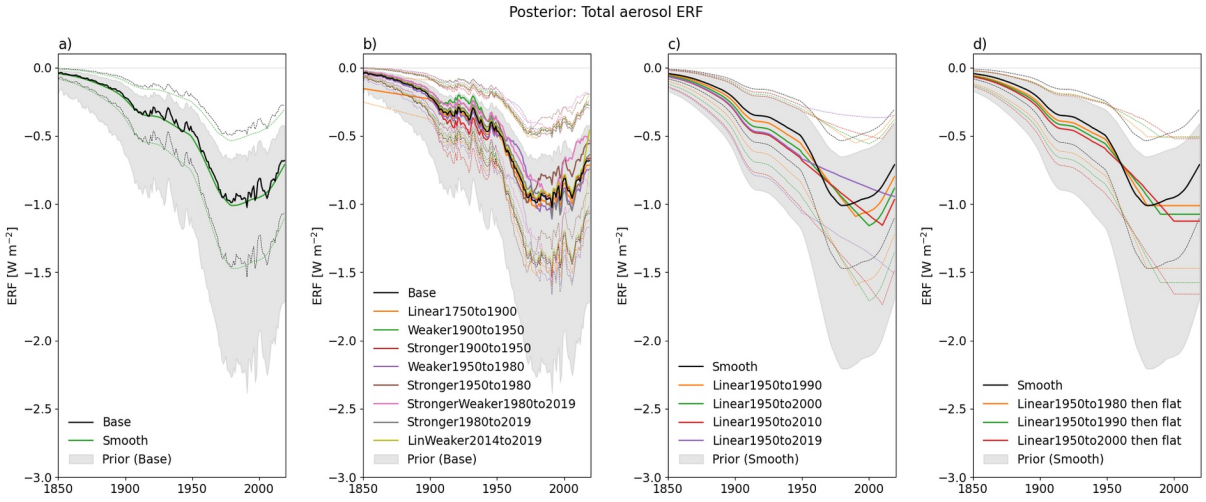

Figure S11: Posterior ERF time series for total aerosol ERF for the sensitivity tests. The mean value is indicated by a thick line and 90% C.I. by dashed lines. The gray shading indicate the 90% C.I. AR6 prior (in a,b) and the smoothed AR6 prior (in c,d) for reference. The priors for the individual tests are presented in Fig. S7.

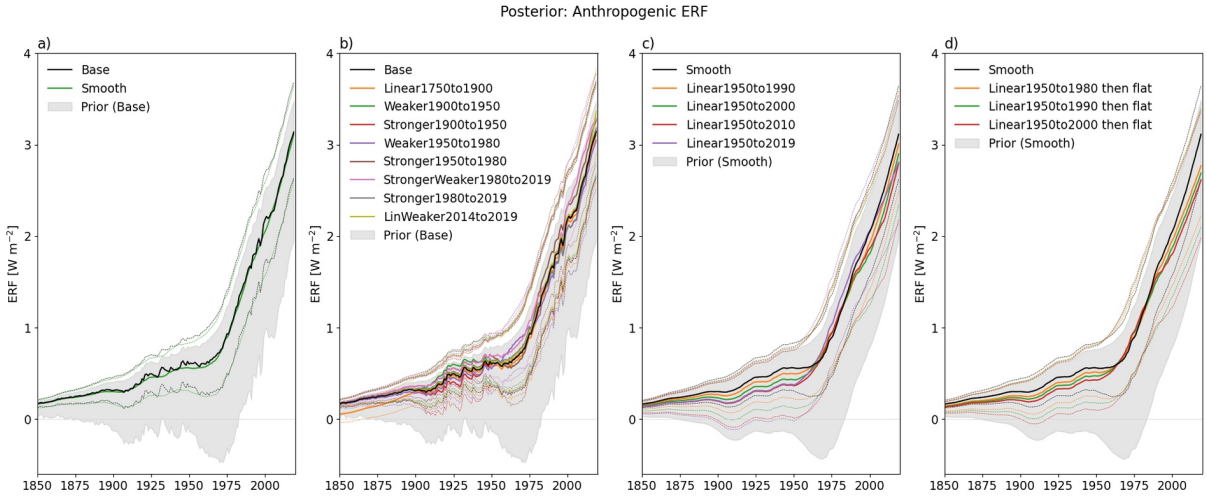

Figure S12: Same as Fig. S11, but for total anthropogenic ERF. The prior for the individual tests are presented in Fig. S8.

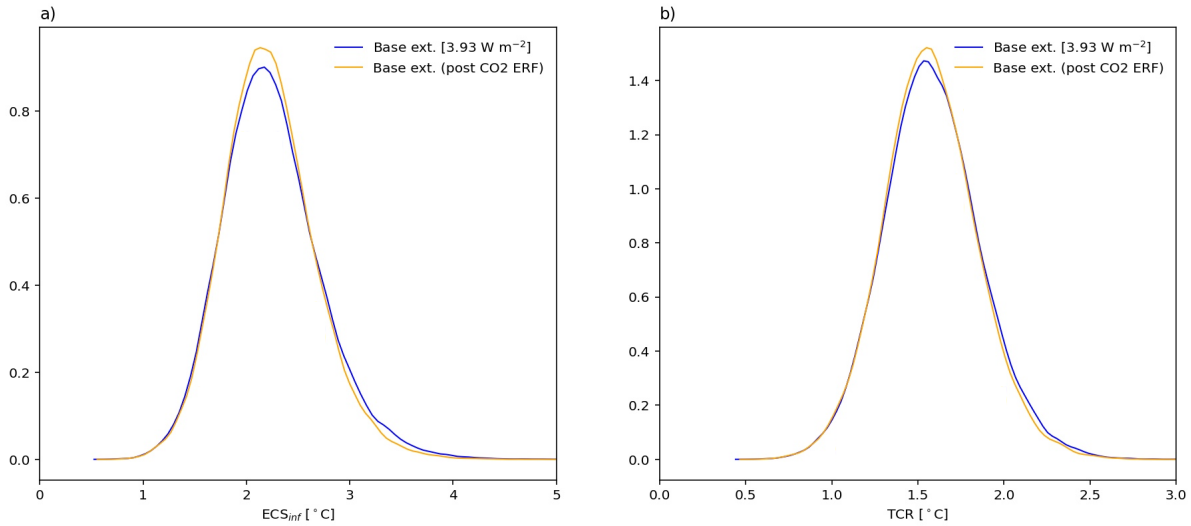

Figure S13: The ECS_{inf} (a) and TCR (b) probability density functions (PDF) for the "Base extended" using the best estimate of 2xCO2 ERF from IPCC AR6 (blue) and the 2xCO2 ERF corresponding to the posterior value of the CO2 ERF in 2022 (orange). To get the 2xCO2 ERF corresponding to the posterior value of CO2 ERF, we scale the AR6 best estimate for 2xCO2 of 3.93 W m^{-2} (Forster et al., 2021) with the ratio of the posteriori value for each ensemble member and the prior mean value for the CO_2 ERF for the end year. Similarly, we use the same scaling factor adjusting the ERF for 1% per year increase in CO_2 concentration used for the TCR calculation.

Supplementary References

Forster, P., T. Storelvmo, K. Armour, W. Collins, J. L. Dufresne, D. Frame, D. J. Lunt, T. Mauritsen, M. D. Palmer, M. Watanabe, M. Wild, and Zhang, H.: The Earth's Energy Budget, Climate Feedbacks, and Climate Sensitivity, in: Climate Change 2021: The Physical Science Basis. Contribution of Working Group I to the Sixth Assessment Report of the Intergovernmental Panel on Climate Change, edited by: Masson-Delmotte, V., P. Zhai, A. Pirani, S. L. Connors, C. Péan, S. Berger, N. Caud, Y. Chen, L. Goldfarb, M. I. Gomis, M. Huang, K. Leitzell, E. Lonnoy, J. B. R. Matthews, T. K. Maycock, T. Waterfield, O. Yelekçi, R. Yu, and Zhou, B., Cambridge University Press, Cambridge, United Kingdom and New York, NY, USA, 2021.

Forster, P. M., Smith, C. J., Walsh, T., Lamb, W. F., Lamboll, R., Hauser, M., Ribes, A., Rosen, D., Gillett, N., Palmer, M. D., Rogelj, J., von Schuckmann, K., Seneviratne, S. I., Trewin, B., Zhang, X., Allen, M., Andrew, R., Birt, A., Borger, A., Boyer, T., Broersma, J. A., Cheng, L., Dentener, F., Friedlingstein, P., Gutiérrez, J. M., Gütschow, J., Hall, B., Ishii, M., Jenkins, S., Lan, X., Lee, J. Y., Morice, C., Kadow, C., Kennedy, J., Killick, R., Minx, J. C., Naik, V., Peters, G. P., Pirani, A., Pongratz, J., Schleussner, C. F., Szopa, S., Thorne, P., Rohde, R., Rojas Corradi, M., Schumacher, D., Vose, R., Zickfeld, K., Masson-Delmotte, V., and Zhai, P.: Indicators of Global Climate Change 2022: annual update of large-scale indicators of the

state of the climate system and human influence, Earth Syst. Sci. Data, 15,2295-2327, 10.5194/essd-15-2295-2023, 2023.

Myhre, G., D. Shindell, F.-M. Bréon, W. Collins, J. Fuglestvedt, J. Huang, D. Koch, J.-F. Lamarque, D. Lee, B. Mendoza, T. Nakajima, A. Robock, G. Stephens, T. Takemura, and Zhang, H.: Anthropogenic and Natural Radiative Forcing, in: Climate Change 2013: The Physical Science Basis. Contribution of Working Group I to the Fifth Assessment Report of the Intergovernmental Panel on Climate Change edited by: Stocker, T. F., D. Qin, G.-K. Plattner, M. Tignor, S.K. Allen, J. Boschung, A. Nauels, Y. Xia, V. Bex, and Midgley, P. M., Cambridge University Press, Cambridge, United Kingdom and New York, NY, USA, 2013.

Skeie, R. B., Berntsen, T., Aldrin, M., Holden, M., and Myhre, G.: Climate sensitivity estimates – sensitivity to radiative forcing time series and observational data, Earth Syst. Dynam., 9,879-894, 10.5194/esd-9-879-2018, 2018.

von Schuckmann, K., Minière, A., Gues, F., Cuesta-Valero, F. J., Kirchengast, G., Adusumilli, S., Straneo, F., Ablain, M., Allan, R. P., Barker, P. M., Beltrami, H., Blazquez, A., Boyer, T., Cheng, L., Church, J., Desbruyeres, D., Dolman, H., Domingues, C. M., García-García, A., Giglio, D., Gilson, J. E., Gorfer, M., Haimberger, L., Hakuba, M. Z., Hendricks, S., Hosoda, S., Johnson, G. C., Killick, R., King, B., Kolodziejczyk, N., Korosov, A., Krinner, G., Kuusela, M., Landerer, F. W., Langer, M., Lavergne, T., Lawrence, I., Li, Y., Lyman, J., Marti, F., Marzeion, B., Mayer, M., MacDougall, A. H., McDougall, T., Monselesan, D. P., Nitzbon, J., Otosaka, I., Peng, J., Purkey, S., Roemmich, D., Sato, K., Sato, K., Savita, A., Schweiger, A., Shepherd, A., Seneviratne, S. I., Simons, L., Slater, D. A., Slater, T., Steiner, A. K., Suga, T., Szekely, T., Thiery, W., Timmermans, M. L., Vanderkelen, I., Wjiffels, S. E., Wu, T., and Zemp, M.: Heat stored in the Earth system 1960–2020: where does the energy go?, Earth Syst. Sci. Data, 15,1675-1709, 10.5194/essd-15-1675-2023, 2023.